Preprint
UCRL-JC-144040

A Split-Step Scheme for the Incompressible Navier-Stokes Equations

W. D. Henshaw, N. A. Petersson

This article was submitted to
Workshop on Numerical Simulations of Incompressible Flows
Half Moon Bay, CA
June 19-21, 2001

June 12, 2001

U.S. Department of Energy

Lawrence
Livermore
National
Laboratory

Approved for public release; further dissemination unlimited

DISCLAIMER

This document was prepared as an account of work sponsored by an agency of the United States Government. Neither the United States Government nor the University of California nor any of their employees, makes any warranty, express or implied, or assumes any legal liability or responsibility for the accuracy, completeness, or usefulness of any information, apparatus, product, or process disclosed, or represents that its use would not infringe privately owned rights. Reference herein to any specific commercial product, process, or service by trade name, trademark, manufacturer, or otherwise, does not necessarily constitute or imply its endorsement, recommendation, or favoring by the United States Government or the University of California. The views and opinions of authors expressed herein do not necessarily state or reflect those of the United States Government or the University of California, and shall not be used for advertising or product endorsement purposes.

This is a preprint of a paper intended for publication in a journal or proceedings. Since changes may be made before publication, this preprint is made available with the understanding that it will not be cited or reproduced without the permission of the author.

This report has been reproduced
directly from the best available copy.

Available to DOE and DOE contractors from the
Office of Scientific and Technical Information
P.O. Box 62, Oak Ridge, TN 37831
Prices available from (423) 576-8401
http://apollo.osti.gov/bridge/

Available to the public from the
National Technical Information Service
U.S. Department of Commerce
5285 Port Royal Rd.,
Springfield, VA 22161
http://www.ntis.gov/

OR

Lawrence Livermore National Laboratory
Technical Information Department's Digital Library
http://www.llnl.gov/tid/Library.html

A Split-Step Scheme for the Incompressible Navier-Stokes Equations

William D. Henshaw
N. Anders Petersson

Centre for Applied Scientific Computing,
Lawrence Livermore National Laboratory,
Livermore, CA, 94551,
henshaw@llnl.gov, andersp@llnl.gov

June 12, 2001

Abstract

We describe a split-step finite-difference scheme for solving the incompressible Navier-Stokes equations on composite overlapping grids. The split-step approach decouples the solution of the velocity variables from the solution of the pressure. The scheme is based on the velocity-pressure formulation and uses a method of lines approach so that a variety of implicit or explicit time stepping schemes can be used once the equations have been discretized in space. We have implemented both second-order and fourth-order accurate spatial approximations that can be used with implicit or explicit time stepping methods. We describe how to choose appropriate boundary conditions to make the scheme accurate and stable. A divergence damping term is added to the pressure equation to keep the numerical dilatation small. Several numerical examples are presented.

1 Introduction

We consider solving the incompressible Navier-Stokes equations with finite difference methods on composite overlapping grids. We describe a split-step (or fractional-step) approach that decouples the solution of the velocity from the solution of the pressure. We describe how to design the method to be accurate and stable. Second-order and fourth-order accuracy has been achieved in space and second or higher order accuracy in time can be easily accomplished.

In primitive-variables the initial-boundary-value problem (IBVP) for the incompressible Navier-Stokes equations is

$$\begin{array}{rcll} \partial\mathbf{u}/\partial t + (\mathbf{u}\cdot\nabla)\mathbf{u} + \nabla p &=& \nu\Delta\mathbf{u} + \mathbf{F}, & \text{for } \mathbf{x}\in\Omega, \quad t>0 \\ \nabla\cdot\mathbf{u} &=& 0, & \text{for } \mathbf{x}\in\overline{\Omega}, \quad t>0 \\ B(\mathbf{u},p) &=& \mathbf{g} & \text{for } \mathbf{x}\in\partial\Omega, \quad t>0 \\ \mathbf{u}(\mathbf{x},0) &=& \mathbf{f}(\mathbf{x}) & \text{for } \mathbf{x}\in\Omega \end{array} \tag{1}$$

Here $\mathbf{u} = (u_1, u_2, u_3)$ is the velocity, p is the pressure, Ω is a bounded open domain in R^d, $d = 2$ or $d = 3$ and $\partial\Omega$ is the boundary of Ω. The initial conditions should satisfy $\nabla\cdot\mathbf{f} = 0$.

There are d boundary conditions denoted by $B(\mathbf{u}, p) = 0$. On a fixed wall, for example, the boundary conditions are $\mathbf{u} = 0$. We assume that all data are sufficiently smooth. Depending on the boundary conditions the pressure may only be determined up to a constant in which case we impose the average pressure to be zero. We refer to the formulation (1) as the "velocity-divergence" formulation.

An alternative form of this IBVP, which we call the "velocity-pressure" formulation, is

$$\begin{array}{rcll} \partial\mathbf{u}/\partial t + (\mathbf{u}\cdot\nabla)\mathbf{u} + \nabla p &=& \nu\Delta\mathbf{u} + \mathbf{F}, & \text{for } \mathbf{x}\in\Omega, \quad t>0 \\ \Delta p + J(\nabla\mathbf{u}) - \alpha(\mathbf{x})\nabla\cdot\mathbf{u} &=& \nabla\cdot\mathbf{F} & \text{for } \mathbf{x}\in\Omega, \quad t\geq 0 \\ B(\mathbf{u},p) &=& \mathbf{g} & \text{for } \mathbf{x}\in\partial\Omega, \quad t>0 \\ \nabla\cdot\mathbf{u} &=& 0 & \text{for } \mathbf{x}\in\partial\Omega \\ \mathbf{u}(\mathbf{x},0) &=& \mathbf{f}(\mathbf{x}) & \text{for } \mathbf{x}\in\Omega \end{array} \tag{2}$$

where

$$J(\nabla\mathbf{u}) = \sum_{m=1}^{d} \nabla u_m \cdot \frac{\partial\mathbf{u}}{\partial x_m}$$

The equation, $\nabla\cdot\mathbf{u} = 0$, for the dilatation in (1) has been replaced by an elliptic equation for the pressure which is obtained by taking the divergence of the momentum equations, and using $\nabla\cdot\mathbf{u} = 0$. Since we have raised the order of the system, this formation requires $d+1$ boundary conditions; an extra boundary condition on the dilatation has been added. The boundary condition $\nabla\cdot\mathbf{u} = 0$ can be thought of as the boundary condition for the pressure equation. We have also added the **divergence damping** term, $\alpha(\mathbf{x})\nabla\cdot\mathbf{u}$, $\alpha\geq 0$, to the pressure equation. Although in the continuous case this term has no effect, in the discrete case this term will be important to keep the dilatation small. To see why this term might be important we can write down the equation satisfied by the dilatation, $\delta = \nabla\cdot\mathbf{u}$, formed by taking the divergence of the momentum equation,

$$\partial\delta/\partial t + (\mathbf{u}\cdot\nabla)\delta = \nu\Delta\delta - \alpha\delta. \tag{3}$$

The term we have added to the pressure equation appears as a linear damping term in the evolution equation for the divergence. Note that $\delta(\mathbf{x},t)$ will be identically zero for all time since the initial conditions are $\delta(\mathbf{x},0) = 0$ and the boundary conditions are $\delta(\mathbf{x},t) = 0$. This observation can be used to show that two formulations (1) and (2) are equivalent, at least for solutions that are sufficiently smooth. We also see the reason for adding boundary condition, $\nabla\cdot\mathbf{u} = 0$, since it forces the dilatation to be zero.

The incompressible Navier-Stokes equations in primitive variables can be discretized in a variety of ways. Harlow and Welch [7] were perhaps the first with the MAC method using staggered grids. Later the projection method was devised by Chorin[4] and independently by Temam[22]. The projection method was extended to an implicit fractional-step method by Kim and Moin[14]. Since that time there have been numerous other approaches developed based on finite-difference, finite-element and spectral-element discretizations, such as [1, 2, 13, 23, 15, 20, 8] to name a few.

There are three fundamental issues that must be dealt with when designing a scheme for the incompressible Navier-Stokes equations:

- The pressure should be free of spurious oscillations. Straight-forward discretizations of (1) can lead to the checker-board instability (corresponding to a violation of the Babuška-Brezzi condition in finite-elements).

- Many approaches require extra boundary conditions, either for the pressure or for an intermediate velocity field, which can be non-trivial to choose.
- If the pressure is only determined up to a constant (for example when Neumann boundary conditions are enforced on $\partial\Omega$), there will be a compatibility condition on the data for the pressure equation.

There have been long discussions in the literature related to these three issues, especially concerning boundary conditions for the pressure [6, 16, 13, 20] and whether fractional-step projection methods are inherently first-order accurate in the pressure [17, 21, 19, 5]. We refer to Brown et. al. [3] for a discussion of how to get second-order accuracy in the pressure with the fractional-step projection method. In this paper, we summarize the results of our research, and describe how the above three issues are handled in our method.

Here we describe a straight-forward approach that leads to an efficient second (or higher) order accurate scheme in both the velocity and the pressure. We use a method of lines approach to discretize the velocity-pressure formulation (2). We begin by discretizing in space. For ease of presentation we consider solving the equations in two dimensions on the unit square, using a rectangular grid, with grid spacing $h = 1/N$, for N a positive integer,

$$\mathbf{G} = \{\mathbf{x_i} = (x_i, y_i) = (ih, jh) \qquad i, j = -1, 0, 1, \ldots, N+1\}$$

Here $\mathbf{i} = (i, j)$ is a multi-index. We include ghost points at the boundaries to aid in the discretization. To be specific we consider a Dirichlet boundary condition for the velocity,

$$\mathbf{u}(\mathbf{x}, t) = \mathbf{g}(\mathbf{x}, t). \tag{4}$$

We first discretize in space. Let $(\mathbf{U_i}(t), P_i(t))$ be the numerical approximation to $(\mathbf{u}(\mathbf{x}, t), p(\mathbf{x}, t))$ with $\mathbf{U_i}(t) = (U_i(t), V_i(t))$. Then the spatial approximation is

$$\begin{aligned}
d\mathbf{U_i}/dt &= -(\mathbf{U_i} \cdot \nabla_h)\mathbf{U_i} - \nabla_h P_i + \nu \Delta_h \mathbf{U_i} + \mathbf{F}(\mathbf{x_i}, t), && i, j = 1, 2, \ldots, N-1 && (5)\\
\Delta_h P_i &= \alpha_i \nabla_h \cdot \mathbf{U_i} - J(\nabla_h \mathbf{U_i}) + \nabla_h \cdot \mathbf{F}(\mathbf{x_i}, t), && i, j = 0, 1, 2, \ldots, N && (6)\\
\mathbf{U_i} &= \mathbf{g}(\mathbf{x_i}, t) \equiv (g^u, g^v)(\mathbf{x_i}, t) && i = 0, j = 0, 1, 2, \ldots, N && (7)\\
D_{0x} U_i &= -D_{0y} g_i^v && i = 0, j = 0, 1, 2, \ldots, N && (8)
\end{aligned}$$

The boundary conditions have only been specified at $x = 0$; similar expressions will hold at the other boundaries. The operators ∇_h, Δ_h are the standard centred difference approximations to ∇ and Δ,

$$\begin{aligned}
\nabla_h \cdot \mathbf{U_i} &= D_{0x}\mathbf{U_i} + D_{0y}\mathbf{U_i} \quad , && \Delta_h \mathbf{U_i} = (D_{+x}D_{-x} + D_{+y}D_{-y})\mathbf{U_i}\\
D_{0x}\mathbf{U_i} &= \frac{\mathbf{U}_{i+1} - \mathbf{U}_{i-1}}{2h} \quad , && D_{0y}\mathbf{U_i} = \frac{\mathbf{U}_{j+1} - \mathbf{U}_{j-1}}{2h}\\
D_{+x}\mathbf{U_i} &= \frac{\mathbf{U}_{i+1} - \mathbf{U}_i}{h} \quad , && D_{-x}\mathbf{U_i} = \frac{\mathbf{U}_i - \mathbf{U}_{i-1}}{h}
\end{aligned}$$

The divergence boundary condition (8) should be thought of as determining the ghost line value of the horizontal velocity component, $U_{-1,j}$. Since we have directly discretized the pressure equation using a compact difference approximation we avoid the checker-board instability problem. The discrete approximation will require extra numerical boundary

conditions. Applying the general principle for deriving numerical boundary conditions described in [12] we use the equations themselves to tell how the solution should behave at the boundary. Note for example, that the pressure equation (6) is applied on the boundary, $i = 0$. As a numerical boundary condition we could also apply the momentum equations on the boundary and thus determine the values for $\mathbf{U}_{-1,j}$. However, in order to keep the solution of the pressure decoupled from the velocity we instead only apply the normal component of the momentum equation on the boundary,

$$\frac{\partial p}{\partial n} = \mathbf{n} \cdot (-\mathbf{g}_t - (\mathbf{g} \cdot \nabla \mathbf{u}) + \nu \Delta \mathbf{u}) \tag{9}$$

and then extrapolate the tangential component of the velocity. We call this the div-grad pressure boundary condition. Note that the boundary condition (9) is just the normal component of the momentum equation applied on the boundary. It adds no new information to the continuous PDE and cannot be used as the extra boundary condition required by the velocity-pressure formulation. It turns out that for implicit time stepping a more stable boundary condition is formed by explicitly removing the dilatation in the highest order term, $\Delta \mathbf{u}$, by using the vector identity

$$\Delta \mathbf{u} = \nabla(\nabla \cdot \mathbf{u}) - \nabla \times \nabla \times \mathbf{u}$$

together with $\nabla(\nabla \cdot \mathbf{u}) = 0$ to give

$$\frac{\partial p}{\partial n} = \mathbf{n} \cdot (-\mathbf{g}_t - (\mathbf{g} \cdot \nabla \mathbf{u}) - \nu \nabla \times \nabla \times \mathbf{u}) \tag{10}$$

We call this the curl-curl boundary condition for the pressure. This boundary condition was apparently first advocated by Karniadakis, Israeli and Orszag [13] as the appropriate boundary condition for the pressure. Unlike equation (9) this new equation does add new information and can be used as an alternative boundary condition to $\nabla \cdot \mathbf{u} = 0$. From our point of view this boundary condition is actually specifying a boundary condition on the normal derivative of the dilatation, $\mathbf{n} \cdot \nabla(\nabla \cdot \mathbf{u}) = 0$, or

$$\frac{\partial}{\partial n}(\nabla \cdot \mathbf{u}) = 0. \tag{11}$$

since (10) was derived from (9) using (11). Referring back to equation (3) we see that the above boundary condition, together with the initial condition $\delta(\mathbf{x}, 0) = 0$, will also force the dilatation to be zero for all time. The stability analysis for this scheme can be found in [18]. The remaining boundary conditions for the discrete scheme are thus a discretization of (10), and extrapolating the tangential component of the velocity,

$$D_{0x} P_{0j} = -\nu D_{+x} D_{-y} V_{0j} \tag{12}$$

$$D^3_{+x} V_{-1j} = V_{-1j} - 3V_{0j} + 3V_{1j} - V_{2j} = 0 \tag{13}$$

Here we have taken $\mathbf{g} = 0$ to show the essential features of the boundary condition. The equations (5-8, 12, 13) can be solved with a method of lines approach. If we wish to have a split-step scheme where the solution of the pressure equation is decoupled from the solution of the velocity components we should choose a time stepping scheme for the velocity components that only involves the pressure from previous time steps. Let us introduce the

operators $L = L_E + L_I$ representing various terms in the momentum equation:

$$L\mathbf{U_i} = -(\mathbf{U_i} \cdot \nabla_h)\mathbf{U_i} - \nabla_h P_\mathbf{i} + \nu \Delta_h \mathbf{U_i} \tag{14}$$

$$L_E\mathbf{U_i} \equiv -(\mathbf{U_i} \cdot \nabla_h)\mathbf{U_i} - \nabla_h P_\mathbf{i} \tag{15}$$

$$L_I\mathbf{U_i} \equiv \nu \Delta_h \mathbf{U_i} \tag{16}$$

L_I and L_E will be the parts of the operator that we will later on treat implicitly and explicitly, respectively.

As a first example we could solve these equations with an explicit multi-step method such as an Adams-Bashforth scheme. In this approach we first advance the velocity using

$$\frac{\mathbf{U}_\mathbf{i}^{n+1} - \mathbf{U}_\mathbf{i}^n}{\Delta t} = \frac{3}{2}(L\mathbf{U}_\mathbf{i}^n + \mathbf{F}_\mathbf{i}^n) - \frac{1}{2}(L\mathbf{U}_\mathbf{i}^n + \mathbf{F}_\mathbf{i}^n) \qquad i,j = 1,2,\ldots,N-1 \tag{17}$$

$$\mathbf{U}_\mathbf{i}^{n+1} = \mathbf{g}(\mathbf{x_i}, t^{n+1}) \qquad i = 0, j = 0,1,\ldots,N \tag{18}$$

$$D_{0x}U_\mathbf{i}^{n+1} = -D_{0y}g_\mathbf{i}^{n+1} \qquad i = 0, j = 0,1,\ldots,N \tag{19}$$

$$D_{+x}^3 V_{-1j}^{n+1} = 0 \qquad j = 0,1,\ldots,N \tag{20}$$

Here $\mathbf{U}_\mathbf{i}^n \approx \mathbf{u}(\mathbf{x_i}, n\Delta t)$. These equations determine $\mathbf{U}_\mathbf{i}^{n+1}$ at all points including the ghost points. We then solve for the pressure from

$$\Delta_h P_\mathbf{i}^{n+1} - \alpha_\mathbf{i} \nabla_h \cdot \mathbf{U}_\mathbf{i}^{n+1} + J(\nabla_h \mathbf{U}_\mathbf{i}^{n+1}) = 0 \qquad i,j = 0,1,2,\ldots,N \tag{21}$$

$$D_{0x}P_{0j}^{n+1} = -\nu D_{+x}D_{-y}V_{0j}^{n+1} \tag{22}$$

In this case one could also use the discrete form of (9)

$$D_{0x}P_{0j}^{n+1} = -\nu D_{+x}D_{-x}U_{0j}^{n+1} \tag{23}$$

instead of (22). To improve the stability properties of the time-integrator, we often use the above scheme as the predictor followed by a second-order Adams-Moulton corrector.

As another example, we have implemented a semi-implicit method that combines a Crank-Nicolson approach for the viscous terms and an Adams-Bashforth approach for the advection terms and pressure. Instead of equation (17) we use

$$\frac{\mathbf{U}^{n+1} - \mathbf{U}^n}{\Delta t} = \frac{3}{2}L_E\mathbf{U}_\mathbf{i}^n - \frac{1}{2}L_E\mathbf{U}_\mathbf{i}^n + \frac{1}{2}(L_I\mathbf{U}_\mathbf{i}^{n+1} + L_I\mathbf{U}_\mathbf{i}^n)$$

together with equations (18-20). Since the boundary condition for the pressure depends on ν/h^2 and since the pressure is taken explicitly in the time stepping scheme it could be that Δt depends on the ratio h^2/ν. This is indeed the case when (9) is used as a boundary condition for the pressure. However, a stability analysis of this method [18] shows that the time step is only determined by the advection terms (.i.e. is independent of ν) if (9) is replaced by the curl-curl boundary condition (10). This is somewhat remarkable, since the pressure is treated explicitly.

It is straight-forward to build time stepping schemes that are accurate to any desired order in time. The reason for this is that in the approach we have taken we have effectively reduced the solution of the incompressible Navier-Stokes equations to solving a system of ODE's for $\mathbf{U_i}$:

$$\frac{d}{dt}\mathbf{U_i} = \mathbf{F}(\mathbf{U_i}, t),$$

since we can treat the pressure simply as a function of the velocity.

The difference approximation presented here can be easily extended to curvilinear grids and to composite overlapping grids. The approximations can be also be made fourth order accurate in space, see [9] for further details.

If the pressure has a Neumann boundary condition on all boundaries the pressure equation will be singular. In order to solve this singular system one could, for example, eliminate one equation and replace it with an equation that, for example, sets the value of p at a point or sets the mean value for p. Rather than single out a particular equation to be removed we prefer to use a different approach which is better conditioned. If we denote the equation for the pressure as the matrix equation,

$$Ax = b \tag{24}$$

then we solve the augmented system

$$\begin{bmatrix} A & r \\ r^T & 0 \end{bmatrix} \begin{bmatrix} x \\ \beta \end{bmatrix} = \begin{bmatrix} b \\ 0 \end{bmatrix}$$

Here r is the right null vector of A, the vector will all components equal to one. This augmented solution will have a unique solution. The last equation will set the mean value of p.

It is important in practice to include the divergence damping term, $\alpha_{\mathbf{i}}\ \nabla_h \cdot \mathbf{U}_{\mathbf{i}}$, in the pressure equation (6). One could alternatively apply an extra explicit projection to the solution after every step, but this would require a significant amount of extra work. The damping coefficient $\alpha(\mathbf{x}, t)$ can be chosen to be quite large. When using an explicit time stepping approach we choose

$$\alpha = C_d\ \nu\ \frac{1}{2}\left(\frac{1}{\Delta x^2} + \frac{1}{\Delta y^2}\right) \tag{25}$$

where the coefficient C_d is usually taken to be about one. On a rectangular grid this makes α proportional to $1/\Delta t$. Note that on a curvilinear grid the coefficient will vary in space. One might wonder whether this divergence damping term, which is a potentially order one addition to the pressure equation, will destroy the accuracy of the method. In [11] we analyse this damping term using normal-mode stability analysis and show that the method retains it's accuracy even with this term. In practice we find that increasing C_d will result in a decrease of the maximum dilatation (up to a point) but also an increase in the error in the pressure.

A von Neumann stability analysis shows that the allowable time step, Δt, will depend on the size of α. For implicit methods we do not want the damping coefficient to significantly reduce the time step so it is necessary to limit the size of α by $C/\Delta t$ for a constant $C = O(1)$.

2 Numerical results

In this section we present some results from a numerical implementation of the scheme described in this paper. The method was implemented in the **OverBlown** flow solver. **OverBlown** is developed using the **Overture** object-oriented framework and can solve the incompressible Navier-Stokes equations on composite overlapping grids in two and three

space dimensions. Both **OverBlown** and **Overture** are freely available from the web. Currently **OverBlown** only has a second-order accurate spatial approximation implemented, although a fourth-order accurate method has previously been developed in Fortran [9].

Details on the discretization and solution procedure, as well as more extensive convergence studies can be found in [10].

As a first test we use the method of analytic solutions to define the following exact solution to the (forced) two-dimensional incompressible Navier-Stokes equations,

$$
\begin{aligned}
u_{\text{true}}(x,y,t) &= (x^2+2xy+y^2)(1+\frac{1}{2}t+\frac{1}{3}t^2)\\
v_{\text{true}}(x,y,t) &= (x^2-2xy-y^2)(1+\frac{1}{2}t+\frac{1}{3}t^2)\\
p_{\text{true}}(x,y,t) &= (x^2+\frac{1}{2}xy+y^2-1)(1+\frac{1}{2}t+\frac{1}{3}t^2)
\end{aligned}
$$

The exact solution is has been chosen to be divergence free which simplifies the implementation. This test example is extremely useful for our purposes since this solution should also an *exact solution to the discrete equations* on a rectangular grid. Indeed the errors obtained when solving this problem are the order of round-off error for grids consisting of a single square and also for a composite grid consisting of a rotated square in a square as shown in table (2). For debugging purposes this is an excellent test since the numerical errors should be exactly "zero" at every time step. It is not necessary to run extensive convergence tests on multiple grids to check convergence rates.

In three dimensions we use the exact solution

$$
\begin{aligned}
u_{\text{true}}(x,y,t) &= (x^2+2xy+y^2+xz)(1+\frac{1}{2}t+\frac{1}{3}t^2)\\
v_{\text{true}}(x,y,t) &= (x^2-2xy-y^2+3xz)(1+\frac{1}{2}t+\frac{1}{3}t^2)\\
w_{\text{true}}(x,y,t) &= (x^2+y^2-2z^2)(1+\frac{1}{2}t+\frac{1}{3}t^2)\\
p_{\text{true}}(x,y,t) &= (x^2+\frac{1}{2}xy+y^2+z^2-1)(1+\frac{1}{2}t+\frac{1}{3}t^2)
\end{aligned}
$$

with results shown in table (2) for a box.

grid	method	$\|p-p_e\|_\infty$	$\|u-u_e\|_\infty$	$\|v-v_e\|_\infty$	$\|w-w_e\|_\infty$	$\|\nabla\cdot\mathbf{u}\|_\infty$
square10	explicit	3.1×10^{-15}	1.8×10^{-15}	8.9×10^{-16}		6.2×10^{-15}
square10	implicit	1.2×10^{-14}	9.8×10^{-15}	3.8×10^{-15}		5.0×10^{-14}
sis	explicit	1.3×10^{-14}	3.6×10^{-15}	3.2×10^{-15}		1.2×10^{-14}
box10	explicit	1.8×10^{-14}	2.7×10^{-15}	1.6×10^{-15}	1.8×10^{-15}	1.6×10^{-14}

Table 1: Maximum errors when the analytic solution is a quadratic polynomial, $\nu = .1$, $t = 1.0$. Since the grids are rectangular the method gives the exact answer to within roundoff. The grid "sis" is the square-in-a-square overlapping grid consisting of a square embedded in a larger square shown in figure (1).

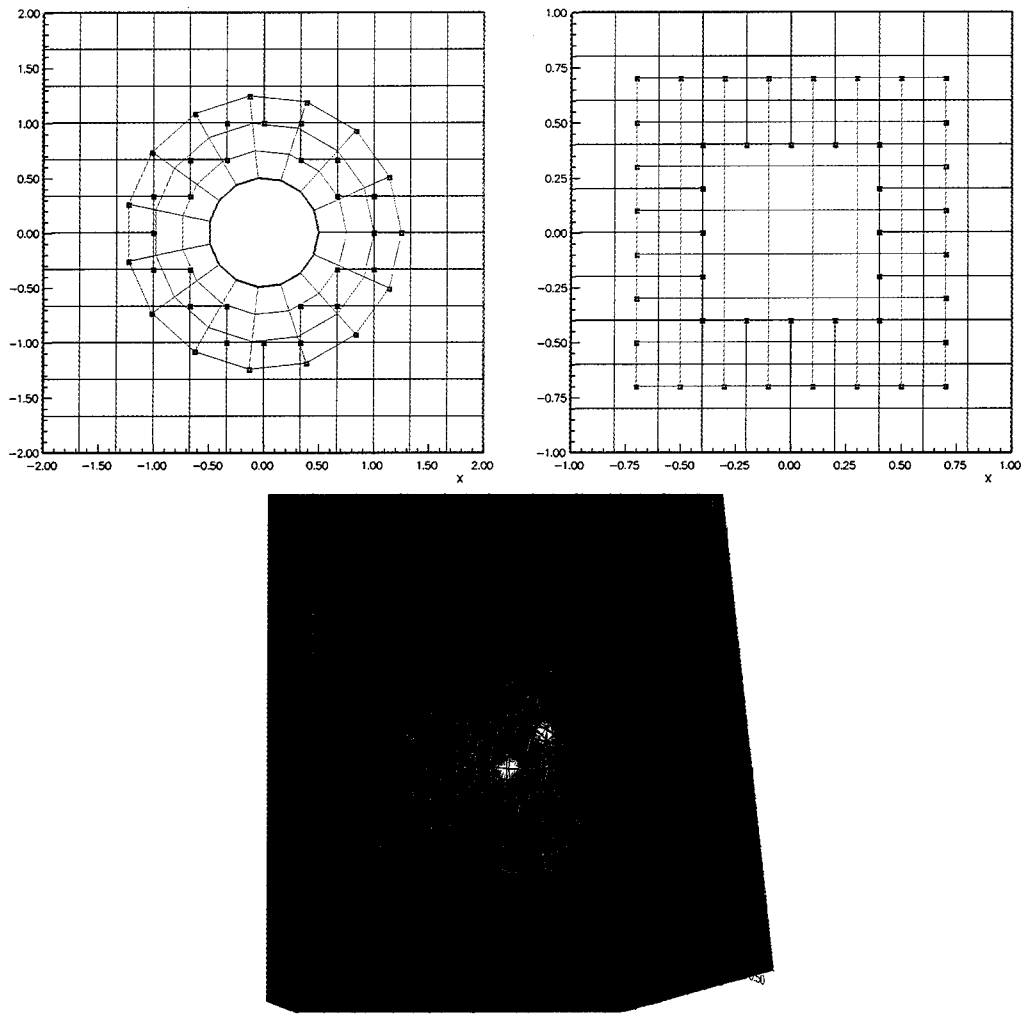

Figure 1: Grids used for the convergence studies: circle-in-a-channel (top-left), square-in-a-square (top right), sphere-in-a-box (bottom left)

Tables (2) and (2) show convergence results when the solution is taken as a trigonometric polynomial. The 2D trigonometric solution used as a twilight zone function is

$$
\begin{aligned}
u_{\text{true}} &= \frac{1}{2}\cos(\pi\omega_0 x)\cos(\pi\omega_1 y)\cos(\omega_3\pi t) + \frac{1}{2} \\
v_{\text{true}} &= \frac{1}{2}\sin(\pi\omega_0 x)\sin(\pi\omega_1 y)\cos(\omega_3\pi t) + \frac{1}{2} \\
p_{\text{true}} &= \cos(\pi\omega_0 x)\cos(\pi\omega_1 y)\cos(\omega_3\pi t) + \frac{1}{2}
\end{aligned}
$$

The 3D trigonometric solution is

$$
\begin{aligned}
u_{\text{true}} &= \cos(\pi\omega_0 x)\cos(\pi\omega_1 y)\cos(\pi\omega_2 z)\cos(\omega_3\pi t) \\
v_{\text{true}} &= \frac{1}{2}\sin(\pi\omega_0 x)\sin(\pi\omega_1 y)\cos(\pi\omega_2 z)\cos(\omega_3\pi t) \\
w_{\text{true}} &= \frac{1}{2}\sin(\pi\omega_0 x)\sin(\pi\omega_1 y)\sin(\pi\omega_2 z)\cos(\omega_3\pi t) \\
p_{\text{true}} &= \frac{1}{2}\sin(\pi\omega_0 x)\cos(\pi\omega_1 y)\cos(\pi\omega_2 z)\sin(\omega_3\pi t)
\end{aligned}
$$

With $\omega_0 = \omega_1 = \omega_2$ it follows that $\nabla \cdot \mathbf{u} = 0$. Values of $\omega_0 = \omega_1 = \omega_2 = 1$ were used in the computations discussed here. At the bottom of the table we show the estimated convergence rates obtained by a least squares fit to the errors.

grid	h_1/h_g	$\|p - p_e\|_\infty$	$\|u - u_e\|_\infty$	$\|v - v_e\|_\infty$	$\|\nabla \cdot \mathbf{u}\|_\infty$
$g = 1$	1	2.4×10^{-1}	1.6×10^{-1}	1.6×10^{-1}	5.0×10^{-1}
$g = 2$	2	5.5×10^{-2}	2.4×10^{-2}	2.5×10^{-2}	1.3×10^{-1}
$g = 3$	4	1.5×10^{-2}	5.0×10^{-3}	4.3×10^{-3}	2.3×10^{-2}
rate		2.0	2.5	2.6	2.2

Table 2: Maximum errors at $t = 1.$ for a trigonometric analytic solution with $\nu = .1$. The domain is discretized by the circle-in-a-channel grid shown in figure (1). The time stepping was a second-order explicit predictor corrector method.

grid	h_1/h_g	$\|p - p_e\|_\infty$	$\|u - u_e\|_\infty$	$\|v - v_e\|_\infty$	$\|w - w_e\|_\infty$	$\|\nabla \cdot \mathbf{u}\|_\infty$
$g = 1$	1	3.3×10^{-1}	1.2×10^{-1}	1.0×10^{-1}	8.8×10^{-2}	4.7×10^{-1}
$g = 2$	2	5.0×10^{-2}	3.6×10^{-2}	3.0×10^{-2}	2.0×10^{-2}	2.3×10^{-1}
$g = 3$	3	2.2×10^{-2}	1.2×10^{-2}	1.2×10^{-2}	9.9×10^{-3}	1.3×10^{-1}
rate		2.5	2.1	1.9	2.0	1.2

Table 3: Maximum errors at $t = 1.$ for a trigonometric analytic solution with $\nu = .05$. The grid is a sphere-in-a-box. The coarse grid, g=1, consists of component grids with $17^3 \bigcup 12 \times 12 \bigcup 12 \times 12$ grid points.

To illustrate the effect that the damping term has on the solution we present some convergence studies. We force the equations so that the true solution is known. In two space dimensions the equations are forced so that the exact solution will be

$$
\begin{aligned}
\mathbf{u}_{\text{true}}(x,y,t) &= \Big(\sin^2(fx)\sin(2fy)\cos(2\pi t)\ ,\ -\sin(2fx)\sin^2(fy)\cos(2\pi t) \Big)\ , \\
p_{\text{true}}(x,y,t) &= \sin(fx)\sin(fy)\cos(2\pi t)\ .
\end{aligned}
$$

We solve the IBVP with and without the damping term turned on. The domain is taken to be the unit square will all boundaries being walls where the velocity is specified. The results for the fourth-order method are given in tables (4) and (5), Indicated are the maximum errors in $\mathbf{u}$, p and $\nabla \cdot \mathbf{u}$. The estimated convergence rate σ, error $\propto h^\sigma$, is also shown. σ is estimated by a least squares fit to the maximum errors given in the table.

The results show that although the methods are converging at the expected rates without the damping term, the errors are significantly reduced when damping term is used.

grid	$\|\mathbf{u}-\mathbf{u}_e\|_\infty$	$\|p-p_e\|_\infty$	$\|\nabla\cdot\mathbf{u}\|_\infty$
20×20	9.3×10^{-4}	8.0×10^{-3}	2.2×10^{-2}
30×30	1.2×10^{-4}	1.4×10^{-3}	2.4×10^{-3}
40×40	2.8×10^{-5}	4.3×10^{-4}	5.1×10^{-4}
rate	5.0	4.2	5.4

Table 4: Maximum errors at $t=1.$ with the 4th order spatial approximation and $\nu=.05$. The divergence damping coefficient is $C_d=1$. Compare these results to table (5) where no divergence damping is used.

grid	$\|\mathbf{u}-\mathbf{u}_e\|_\infty$	$\|p-p_e\|_\infty$	$\|\nabla\cdot\mathbf{u}\|_\infty$
20×20	2.4×10^{-3}	1.3×10^{-2}	6.4×10^{-2}
30×30	5.1×10^{-4}	2.5×10^{-3}	1.3×10^{-2}
40×40	1.7×10^{-4}	8.2×10^{-4}	4.4×10^{-3}
rate	3.8	4.0	3.9

Table 5: Maximum errors at $t=1.$ with the 4th order spatial approximation and $\nu=.05$. The divergence damping coefficient is $C_d=0$. Compare these results to table (4) where divergence damping is used.

To illustrate the benefits of using the curl-curl boundary condition (10) we compare the numerically determined largest stable time-step for the implicit time-stepping scheme in table (6). The allowable time step for the curl-curl boundary condition is independent of ν/h^2 so that Δt only depends on the advection terms (which are treated explicitly). In contrast the div-grad boundary condition (9) requires a Δt that depends on ν/h^2.

BC	Grid	Δt	$\|p-p_e\|_\infty$	$\|u-u_e\|_\infty$	$\|v-v_e\|_\infty$	$\|\nabla\cdot\mathbf{u}\|_\infty$
div-grad	coarse	$2.0\cdot 10^{-3}$	$5.8\cdot 10^{-2}$	$4.2\cdot 10^{-2}$	$8.6\cdot 10^{-2}$	$1.1\cdot 10^{-1}$
div-grad	fine	$5.0\cdot 10^{-4}$	$5.7\cdot 10^{-3}$	$8.8\cdot 10^{-3}$	$1.5\cdot 10^{-2}$	$2.4\cdot 10^{-2}$
curl-curl	coarse	$1.1\cdot 10^{-2}$	$5.8\cdot 10^{-2}$	$4.2\cdot 10^{-2}$	$8.6\cdot 10^{-2}$	$1.1\cdot 10^{-1}$
curl-curl	fine	$5.5\cdot 10^{-3}$	$5.8\cdot 10^{-3}$	$8.8\cdot 10^{-3}$	$1.5\cdot 10^{-2}$	$2.4\cdot 10^{-2}$

Table 6: A comparison of the div-grad boundary condition (9) and the curl-curl boundary condition (10). Shown are the largest stable time-steps and maximum errors for a forced computation. The time-step for the the curl-curl boundary condition can be chosen much larger since it is does not depend on the ratio ν/h^2. The grid is a circle-in-a-channel. The coarse grid had $41\times 21\cup 21\times 14$ points and the fine grid had $81\times 41\cup 41\times 27$ points.

As an illustration of some more advanced applications of our approach, in figure (2) we show the solution to an incompressible flow containing two rigid cylinders. The cylinders fall under the influence of gravity and their motion is altered by the forces exerted by the fluid. In this computation the overlapping grids are recomputed at every time step. Figure (3) shows the flow past a rotating disk. Figure (4) shows the flow past a wing and flap.

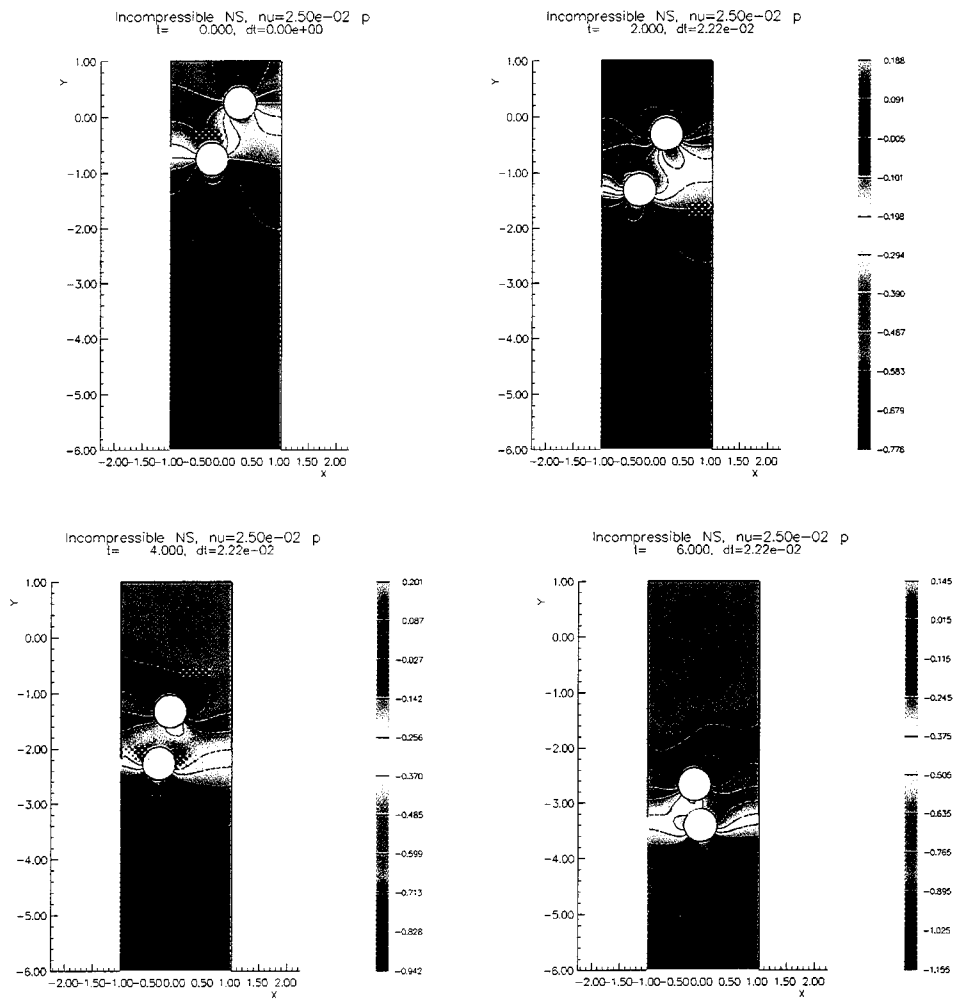

Figure 2: Two falling bodies in an incompressible flow.

3 Software availability

The **OverBlown** flow solver and **Overture** are freely available from the web at `http://www.llnl.gov/casc/Overture`.

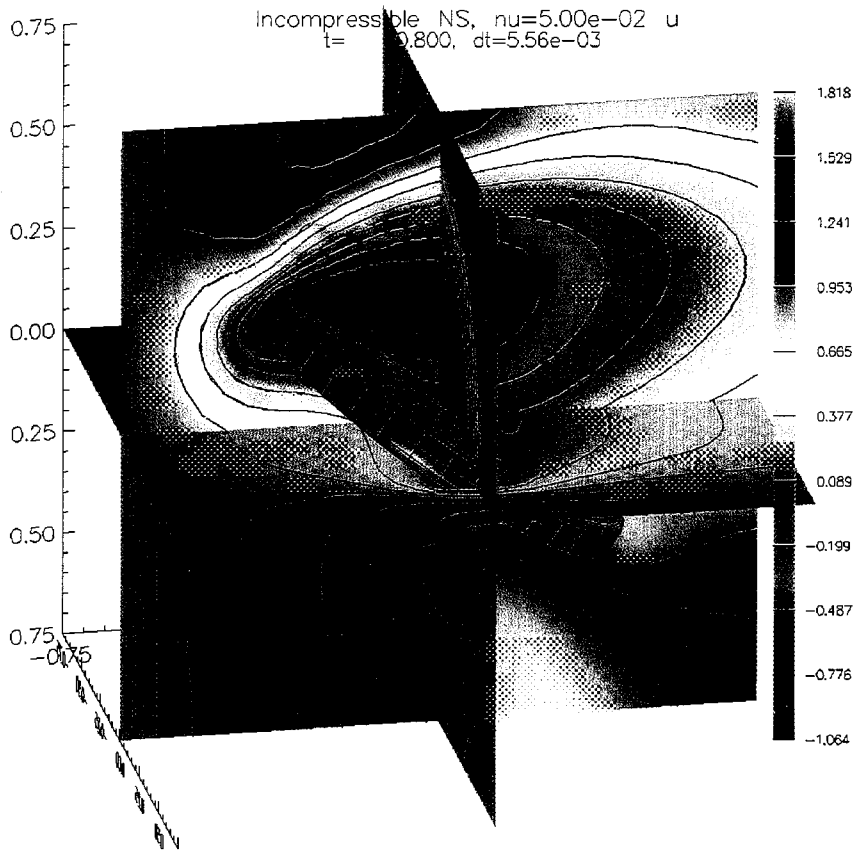

Figure 3: Flow past a rotating disk.

References

[1] S. Abdallah, *Numerical solutions for the pressure poisson equation with Neumann boundary conditions using a non-staggered grid, I*, J. Comp. Phys., 70 (1987), pp. 182–192.

[2] J. B. Bell, P. Colella, and H. M. Glaz, *A second-order projection method for the incompressible navier-stokes equations*, J. Comp. Phys., 85 (1989), pp. 257–283.

[3] D. L. Brown, R. Cortez, and M. L. Minion, *Accurate projection methods for the incompressible Navier–Stokes equations*, J. Comp. Phys., 168 (2001), pp. 464–499.

[4] A. J. Chorin, *Numerical solution of the Navier-Stokes equations*, Math. Comp., 22 (1968), pp. 745–762.

[5] W. E and J. Guo Liu, *Projection method II: Godunov-Ryabenki analysis*, Siam J. of Numer. Anal., 33 (1996), pp. 1597–1621.

[6] P. M. Gresho and R. L. Sani, *On the pressure boundary conditions for the incompressible Navier-Stokes equations*, International Journal for Numerical Methods in Fluids, 7 (1987), pp. 1111–1145.

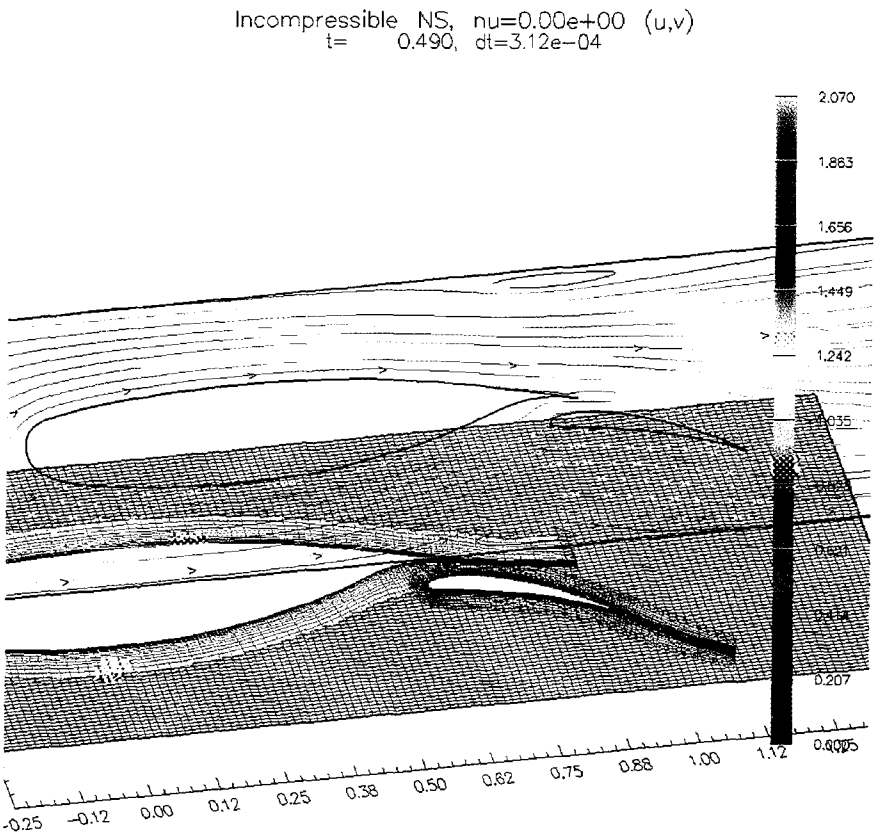

Figure 4: Flow past a wing and flap.

[7] F. HARLOW AND J. WELCH, *Numerical calculation of time-dependent viscous incompressible flow of fluid with free surface*, J. Comp. Phys., 8 (1965), pp. 2182–2189.

[8] W. HEINRICHS, *Splitting techniques for the unsteady stokes equations*, SIAM J. of Numer. Anal., 35 (1998), pp. 1646–1662.

[9] W. HENSHAW, *A fourth-order accurate method for the incompressible Navier-Stokes equations on overlapping grids*, Journal of Computational Physics, 113 (1994), pp. 13–25.

[10] ——, *OverBlown: A fluid flow solver for overlapping grids, user guide*, Research Report UCRL-MA-134288, Lawrence Livermore National Laboratory, 1999.

[11] W. HENSHAW AND H.-O. KREISS, *Analysis of a difference approximation for the incompressible navier-stokes equations*, Research Report LA-UR-95-3536, Los Alamos National Laboratory, 1995.

[12] W. HENSHAW, H.-O. KREISS, AND L. REYNA, *A fourth-order accurate difference approximation for the incompressible Navier-Stokes equations*, Computers and Fluids, 23 (1994), pp. 575–593.

[13] G. KARNIADAKIS, M. ISRAELI, AND S. A. ORSZAG, *High-order splitting methods for the incompressible Navier-Stokes equations*, J. Comp. Phys., 97 (1991), pp. 414–443.

[14] J. KIM AND P. MOIN, *Application of a fractional-step method to incompressible Navier-Stokes equations*, J. Comp. Phys., 59 (1985), pp. 308–323.

[15] K. KORCZAK AND A. T. PATERA, *An isoparametric spectral element method for solution of the Navier-Stokes equations in complex geometry*, J. Comp. Phys., 62 (1986), pp. 361–382.

[16] S. A. ORSZAG, M. ISRAELI, AND M. O. DEVILLE, *Boundary conditions for incompressible flows*, Journal of Scientific Computing, 1 (1986), pp. 75–111.

[17] J. B. PEROT, *An analysis of the fractional step method*, J. Comput. Phys., 108 (1993), pp. 51–58.

[18] N. A. PETERSSON, *Stability of pressure boundarey conditions for stokes and navier-stokes equations*, Research Report UCRL-JC-137733, Lawrence Livermore National Laboratory, 2000. To appear JCP.

[19] J. SHEN, *On error estimates of the projection methods for the Navier-Stokes equations: second-order schemes*, Math. Comp., 65 (1996), pp. 1039–1065.

[20] J. STRIKWERDA, *Finite difference methods for the Stokes and Navier-Stokes equations*, SIAM J. Sci. Stat. Comput., 5 (1984), pp. 56–68.

[21] J. C. STRIKWERDA AND Y. S. LEE, *The accuracy of the fractional step method*, SIAM J. Numer. Anal., 37 (1999), pp. 37–47.

[22] R. TEMAM, *Sur l'approximation de la solution des equation de Navier-Stokes par la méthode des fractionnarires ii*, Arch. Rational Mech. Anal., 33 (1969), pp. 377–385.

[23] J. A. WRIGHT AND W. SHYY, *A pressure-based composite grid method for the Navier-Stokes equations*, J. Comp. Phys., 107 (1993), pp. 225–238.

This work was performed under the auspices of the U.S. Department of Energy by the University of California, Lawrence Livermore National Laboratory under Contract No. W-7405-Eng-48.